Joint Centre for Mesoscale Meteorology, Reading, UK

Superposing Semi-Geostrophic Potential Vorticity Anomalies

A. J. Thorpe
H. R. Birkett

Internal Report No. 76

September 1997

Met Office Joint Centre for Mesoscale Meteorology Department of Meteorology
University of Reading PO Box 243 Reading RG6 6BB United Kingdom
Tel: +44 (0)118 931 8425 Fax: +44 (0)118 931 8791
www.metoffice.com

Designed and produced by the Met Office © Crown copyright 2001 01/0240 The Met Office logo is a registered trademark.

Superposing Semi-Geostrophic Potential Vorticity Anomalies

H. R. Birkett and A. J. Thorpe
Department of Meteorology, University of Reading

Summary

A numerical method for inversion of the semi-geostrophic potential vorticity equation is described. It is used to examine the validity of a strictly linear superposition principle when applied to this high order balance model. These results are important when aiming to extend rigorously the value of recent 'attribution' ideas. Experiments conclude that the non-linear components of the inversion have only a very short-range effect with a magnitude which increases with the magnitude of the potential vorticity anomalies.

For balance of higher-order than quasi-geostrophic these results show that, whilst flow and temperature of an anomaly are non-linear functions of PV magnitude, spatially separated anomalies are quasi-linearly superposable.

Keywords: potential vorticity, semi-geostrophic equations, attribution.

1. Introduction

Recently ideas of 'attribution' have been proposed to describe the individual contributions of various forcing mechanisms in the generation of cyclonic storms ((Davis and Emanuel (1991), Davis (1992), Bishop and Thorpe (1994), Thorpe and Bishop (1995)). It involves dividing the atmosphere in terms of a collection of potential vorticity (PV) anomalies. Each anomaly has associated with it a unique geopotential field analogous to the induction of an electric field, by an electric charge. This field can be obtained by inverting the PV equation for given boundary conditions. The electrostatics analogy and 'action-at-a-distance' have been discussed in Bishop and Thorpe (1994) for quasi-geostrophic PV and extended to the Ertel-Rossby formulation in Thorpe and Bishop (1995).

One of the attractive aspects of quasi-geostrophic PV inversion is its linearity. A consequence of this is that the flow and temperature derived from the geopotential field attributed to individual anomalies are also linear functions, and therefore can be simply added together i.e. a linear superposition principle. It is only under these conditions that the concept of attribution is a linear one. However quasi-geostrophic PV and its inversion have severe limitations particularly as the Rossby number approaches unity. Higher order approximations to PV inherently involve a non-linearity which means that a strictly linear superposition principle will not apply. This is a complication which in principle could limit the usefulness of PV-thinking as applied to real atmospheric flows. However if the consequences of the nonlinear terms can be shown to be small then it may still be a useful concept to explore. Here we assess quantitatively how significant this non-linearity of superposition is for semi-geostrophic PV inversion.

To illustrate the non-linearity in the superposition imagine a given PV anomaly to be composed of the sum of two exactly overlapping anomalies each of half the amplitude. Since the flow and temperature field is not a *linear* function of the magnitude of the anomaly, superposing the solutions will give a different field to that obtained by inverting a single anomaly of the whole amplitude. The non-linearity can be evaluated by performing an inversion for the full anomaly and then subtracting the result of a linear superposition of the inversion of the two sub-anomalies from which we imagine the full anomaly to be composed. In the limit of the two anomalies being removed very far apart, the linear superposition principle would be exact since the fields created by each no longer interact. If the non-linearity decreases rapidly as the distance between the two anomalies increases then the linear superposition principle can, for all practical purposes, be retained for spatially distinct anomalies. It would then only be necessary to account for the nonlinear dependence of the flow and temperature on the PV amplitude of each anomaly alone.

In this note we quantify the superposability by finding the full non-linear inversion solutions for anomalies of varying sizes and magnitudes.

2. Semi-geostrophic analytical solution.

As discussed in Thorpe and Bishop (1995) the semi-geostrophic PV can be written as a function of the geopotential ϕ' in the following way if (and only if) the PV anomaly has a radial symmetry:

$$s' = \frac{1}{f r^2}\frac{\partial}{\partial r}\left(r^2 \frac{\partial \phi'}{\partial r} + \frac{1}{f^2} r \left(\frac{\partial \phi'}{\partial r}\right)^2 + \frac{1}{3f^4}\left(\frac{\partial \phi'}{\partial r}\right)^3 \right) \tag{1}$$

where s′ is the potential vorticity (or more accurately the potential vorticity substance) anomaly suitably normalised to have the dimensions of vorticity and embedded in a motionless infinite atmosphere with constant static stability N^2 and Coriolis parameter f, and $r = \left(x^2 + y^2 + \frac{N^2}{f^2} z^2 \right)^{1/2}$ is a radial coordinate centred on the anomaly.

Solutions for a localised ball (radius r_o) of semi-geostrophic potential vorticity of uniform strength s_o, can be found in terms of the geopotential gradient, $\partial\phi'/\partial r$:

$$\begin{aligned} \frac{\partial \phi'}{\partial r} &= f^2 r \left(\left(1 + \frac{s_o}{f}\frac{r_o^3}{r^3} \right)^{1/3} - 1 \right) \qquad r > r_o \\ \frac{\partial \phi'}{\partial r} &= f^2 r \left(\left(1 + \frac{s_o}{f} \right)^{1/3} - 1 \right) \qquad r < r_o \end{aligned} \tag{2}$$

and analytical solutions for temperature and wind can be found directly from these equations since

$$u = -\frac{1}{f}\frac{\partial \phi'}{\partial y}, \quad v = \frac{1}{f}\frac{\partial \phi'}{\partial x}. \tag{3}$$

$$\theta = \theta' + \bar{\theta}$$

where θ′ is the potential temperature perturbation due to the anomaly and $\bar{\theta}$ is the potential temperature due to the atmospheric lapse rate as given by:

$$\frac{\partial \phi'}{\partial z} = \frac{g\theta'}{\theta_o}, \quad \frac{d\bar{\theta}}{dz} = \frac{\theta_o N^2}{g} \tag{4}$$

The *non-linear* dependence of, say, the θ field on PV magnitude can be seen in:

$$\begin{aligned} \theta &= \theta_o \left(1 + \frac{N^2}{g} z \left(1 + \frac{s_o}{f}\frac{r_o^3}{r^3} \right)^{1/3} \right) \qquad r > r_o \\ \theta &= \theta_o \left(1 + \frac{N^2}{g} z \left(1 + \frac{s_o}{f} \right)^{1/3} \right) \qquad r < r_o \end{aligned} \tag{5}$$

These *analytical* solutions can be used to test the validity of numerical solutions.

3. Semi-geostrophic numerical solution for a single anomaly

To consider superposition of two (or more) anomalies it is necessary to create a more general method of solution for the PV inversion equation i.e. a *numerical* solution. In Cartesian coordinates equation (1) can be written:

$$
\left.\begin{aligned}
s' = \frac{1}{f}\left(\phi'_{xx} + \phi'_{yy} + \frac{f^2}{N^2}\phi'_{zz}\right) \\
+\frac{1}{fN^2}\left(\left(\phi'_{xx} + \phi'_{yy}\right)\phi'_{zz} - \phi'^2_{xz} - \phi'^2_{yz}\right) \\
+\frac{1}{f^3}\left(\phi'_{xx}\phi'_{yy} - \phi'^2_{xy}\right) \\
+\frac{1}{f^3N^2}\det\begin{bmatrix} \phi'_{xx} & \phi'_{xy} & \phi'_{xz} \\ \phi'_{xy} & \phi'_{yy} & \phi'_{yz} \\ \phi'_{xz} & \phi'_{yz} & \phi'_{zz} \end{bmatrix}
\end{aligned}\right\} = Q.-G.
$$

$$
\left.\begin{aligned}
&+\frac{1}{fN^2}\left(\left(\phi'_{xx} + \phi'_{yy}\right)\phi'_{zz} - \phi'^2_{xz} - \phi'^2_{yz}\right) \\
&+\frac{1}{f^3}\left(\phi'_{xx}\phi'_{yy} - \phi'^2_{xy}\right) \\
&+\frac{1}{f^3N^2}\det\begin{bmatrix} \phi'_{xx} & \phi'_{xy} & \phi'_{xz} \\ \phi'_{xy} & \phi'_{yy} & \phi'_{yz} \\ \phi'_{xz} & \phi'_{yz} & \phi'_{zz} \end{bmatrix}
\end{aligned}\right\} non-linear\ terms = b(\phi') \qquad (6)
$$

where subscripts indicate partial derivatives.

The first (and dominant) part of this equation is exactly equal to the incompressible quasi-geostrophic approximation which can be solved numerically via a Poisson solver. A NAG routine for solving the Helmholtz equation (constant λ=0) is used here and we define our domain as a box 2000x2000x20km, with boundary conditions ϕ'=0 on lateral boundaries, and $\partial\phi'/\partial z = 0$ (θ'=0) on horizontal boundaries. The potential vorticity anomaly was defined, for simplicity of analytical solution (shown above), as a ball with radius 200km.

By solving the quasi-geostrophic PV equation using a PV amplitude of s_o, a 'first guess' approximation to the geopotential, ϕ_1', can be found. By feeding this ϕ_1' into the 'nonlinear' terms a quantity s'_1 can be evaluated:

$$s'_1 = s_o - b(\phi_1')$$

where b is a function given in equation (6). Using this s'_1 as the PV source a new value of the quasi-geostrophic geopotential ϕ_2' could then be generated and a new field $b(\phi_2')$ calculated. Again

$$s'_2 = s_o - b(\phi_2')$$

s_o as defined above. To get rapid convergence the solution after each iteration was averaged with the previous solution before the next iteration was performed. This iteration procedure converges to the semi-geostrophic solution, and the value of the geopotential at each point could be used to generate potential temperature and velocity fields. From these, rigorous comparisons with the analytical solutions could be made.

The numerical solution can be made as close to the analytical solution as required for accuracy by increasing the resolution at the expense only of run time. At higher resolution and for large amplitude anomalies (i.e. where two anomalies overlap) convergence was more difficult to reach and a method involving the relaxation of the $b(\phi'_i)$ field for the first five iterations was developed to counteract initial rapid divergence.

4. Superposition of potential vorticity anomalies

To assess the error inherent in linearly superposing solutions from a *non-linear* inversion two different methods of determining the flow due to two semi-geostrophic potential vorticity ball anomalies were compared. The same model domain was used and each anomaly had radius 200km.

- The first method was to produce two separate inversions for PV balls 1 and 2 where ball one was centred in the left hand half of the domain and ball two in the right hand side, each centred at the

same height and at an equal distance from the left and right boundaries respectively. The velocity and θ fields produced separately for each were then added together to produce a 'linear superposition inversion' (denoted 3) of the two balls together.

- Secondly the same two anomalies were included in the domain together and a 'complete inversion' (denoted 4) was performed using the numerical method developed.

This experiment was conducted four times, twice as above, and twice with vertical rather than horizontal alignment, for the anomalies. In the first and third experiments the anomalies had equal magnitude $4\text{x}10^{-4}\text{s}^{-1}$, and in the second and fourth experiments the anomalies had equal and *opposite* magnitude $0.9\text{x}10^{-4}\text{s}^{-1}$, and $-0.9\text{x}10^{-4}\text{s}^{-1}$. These results were then compared by producing graphical representations of the flow, velocity field, and potential temperature pattern , and also, by differencing the two sets of fields produced, as below:

Maximum θ difference = $\left|\left(\theta_4-\theta_3\right)_{\text{max.}}\right|$ where $\theta_3=\theta_1+\theta_2-\left(\theta_o\left(1+\frac{N^2}{g}z\right)\right)$,

maximum velocity difference = $\left|\left(v_4-v_3\right)_{\text{max.}}\right|$ where $v_3=v_1+v_2$,

normalised θ difference= $\left|\frac{\left(\theta_4-\theta_3\right)_{\max}}{\theta'_{4\max}}\right|$ where $\theta'_{4\max}=\left(\theta_4-\theta_o\left(1+\frac{N^2}{g}z\right)\right)_{\max}$,and

normalised velocity difference = $\left|\frac{\left(v_4-v_3\right)_{\max}}{v_{4\max}}\right|$

where $(\theta_o(1+N^2z/g)$ is the background potential temperature distribution and this must be subtracted off to obtain the potential temperature anomaly due to the PV anomaly only. Throughout this paper N^2 is assumed constant and equal to $1\text{x}10^{-4}\text{s}^{-2}$, similarly the Coriolis parameter f = $1\text{x}10^{-4}\text{s}^{-1}$).

This procedure was repeated for anomalies at varying distances apart, (as measured by the distance between the centres of the two anomalies) such that the distance apart divided by the diameter of the anomalies decreased from 3 to 0. For overlapping anomalies the 'complete inversion' was performed for an anomaly of $8\text{x}10^{-4}\text{s}^{-1}$ in the regions of overlap and for $4\text{x}10^{-4}\text{s}^{-1}$ otherwise.

Experiments five and six were performed varying the magnitude of the anomalies from $-1\text{x}10^{-4}\text{s}^{-1}$ to $4\text{x}10^{-4}\text{s}^{-1}$ whilst keeping the distance apart horizontally and vertically respectively, constant at 1.5 diameters.

5. Results and Conclusion

The results of these experiments are shown in figures 1 to 4. Figure 1 shows the difference field for potential temperature with anomalies a distance apart equal to 1.5 diameters, radius 200km for the four experimental cases. Figures 1b) and d) show that for one anomaly negative and the other positive the maximum error occurs near or coincident with the negative anomaly. This follows from the greater effect a single negative anomaly has upon the field than a single positive anomaly of the same magnitude. Figures 1 a) and c) show that for both anomalies magnitude 4f the maximum error occurs symmetrically between the PV spheres. For both vertically aligned cases the maximum error is in fact coincident with one or both of the anomalies, rather than between as for the horizontal cases.

An overall picture of the error in linearly superposing anomalies can be seen in figures 2 and 3. Figure 2 shows the maximum error in all four cases, and figure 3 shows the percentage (or normalised) error in the four cases. For spatially distinct anomalies (i.e. distance apart/diameter of anomalies greater than one) the error remains negligible, around 7.5% of the maximum values of the anomalous potential temperature and velocity at most, and this decreases with increasing separation. The rapid spatial decay of the non-linearities is anticipated in Thorpe and Bishop (1995) in their analysis of the spatial dependence

of the semi-geostrophic "dielectric constant". For experiments with s_0=4f, as the anomalies approach each other the error increases rapidly, reaching a maximum error of around 30% for complete overlap. This "overlap" error in linear superposition can be seen, from equation (5), to be due to the non-linear dependence of ϕ' or potential temperature on the magnitude of the PV anomaly. The error is approximately similar in both the velocity and potential temperature fields. For experiments with s_0=0.9f and -0.9f the percentage difference becomes unbounded since the 'complete inversion' has both zero velocity and zero potential temperature perturbation associated with it, and the error in making a linear superposition is the maximum possible. On the other hand figures 3b) and d) show that the error in linear superposition falls off even more rapidly as the anomalies of opposite sign are moved apart. These results have implications when wishing to divide a distinct anomaly into more easily describable or invertible shapes. Similar results were obtained for anomalies of half the radius although percentage errors were slightly reduced.

Figure 4 shows results from experiments changing the magnitude of the anomalies whilst they remain 1.5 diameters apart in both the horizontal and vertical direction. It can be seen that the amplitude has a strong influence on the error, with a near-linear variation in percentage difference so that linear superposition is a better approximation for smaller magnitude anomaly inversions. However for negative anomalies the error increases greatly near to -f , although still remaining below 5%. This dependence can be described analytically for ball-shaped semi-geostrophic PV anomalies, as shown by Thorpe and Bishop (1995).

Quasi-geostrophic equations are widely used to determine the effects of potential vorticity anomalies, and the method of attribution has been developed with this in mind. However there are many situations in which quasi-geostrophic theory is not applicable and a more accurate approximation is required. These results show that attribution ideas can also be extended to semi-geostrophic theory, with a few qualifications. It is clear that the non-linear component of the semi-geostrophic inversion does indeed have a very short-range effect as hypothesised by Thorpe and Bishop (1995).

In this paper we have used idealised PV anomalies so that simple conclusions can be made. These results show that for balance of higher-order than quasi-geostrophic, flow and temperature of an anomaly are non-linear functions of PV magnitude whilst spatially separated anomalies are quasi-linearly superposable. It is important that these conclusions be used to interpret superposition for the more complex structure of PV anomalies observed in the atmosphere.

References

Bishop, C.H. and Thorpe, A.J.	1994	Potential vorticity and the electrostatics analogy: Quasi-geostrophic theory. *Q. J. R. Meteorol. Soc.*, **120**, 713-731
Davis, C.	1992	Piecewise Potential Vorticity Inversion. *J. Atmos. Sci.*, **49**, 1397-1411
Davis, C. and Emanuel, K.A.	1991	Potential vorticity diagnostics of cyclogenesis. *Mon. Weather Review*, **119**, 1929-1953
Thorpe, A.J. and Bishop, C.H.	1995	Potential vorticity and the electrostatics analogy: Ertel-Rossby formulation. *Q. J. R. Meteorol. Soc.*, **121**, 1477-1495

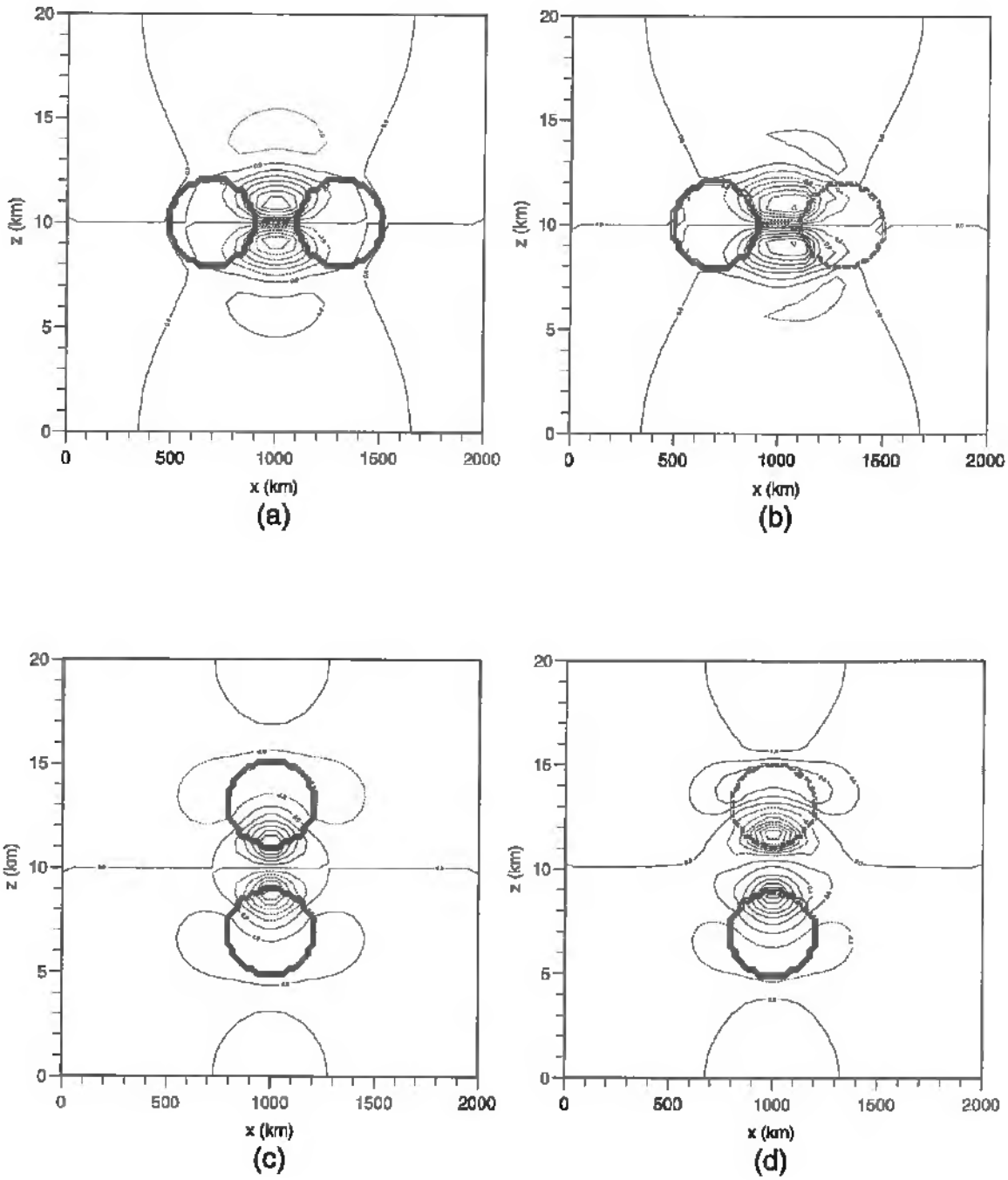

Fig 1 Difference in potential temperature field and full linearly superposed inversion solutions for anomalies whose centres are 1.5 diameters apart a) horizontally aligned and magnitude 4f, b) horizontally aligned and magnitudes 0.9f and -0.9f, c) vertically aligned and magnitude 4f, and d) vertically aligned and magnitudes 0.9f and -0.9f. (Values multiplied by 100, contour interval 0.04°K, negative contours dashed). Position of anomalies also marked in bold lines (Contour interval $0.8\times10^{-4}s^{-1}$ for a) and c), $0.4\times10^{-4}s^{-1}$ for b) and d)).

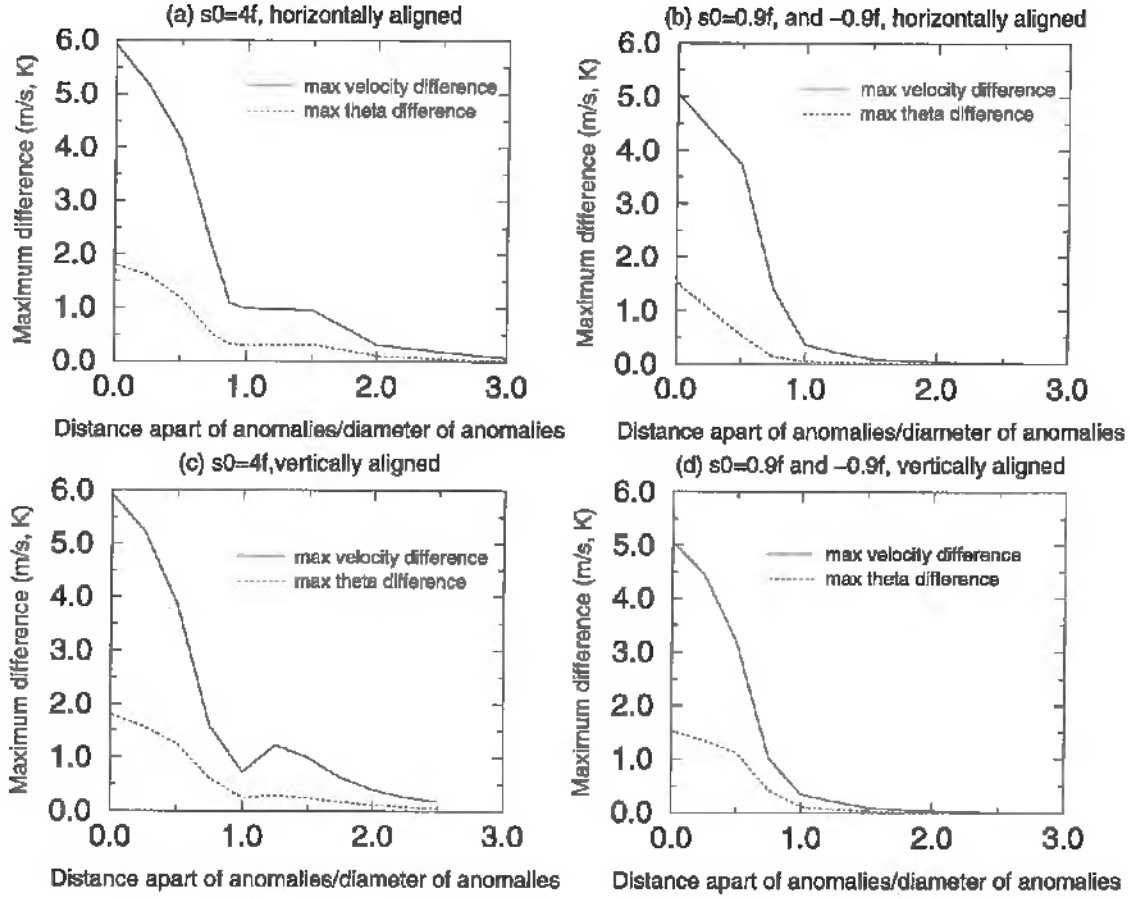

Fig 2: Maximum difference between linearly superposed and full solutions for two anomalies at different distances apart with alignment and magnitude as stated on each graph. Note: the distance apart of the anomalies refers to the distance between the centres of the two anomalies.

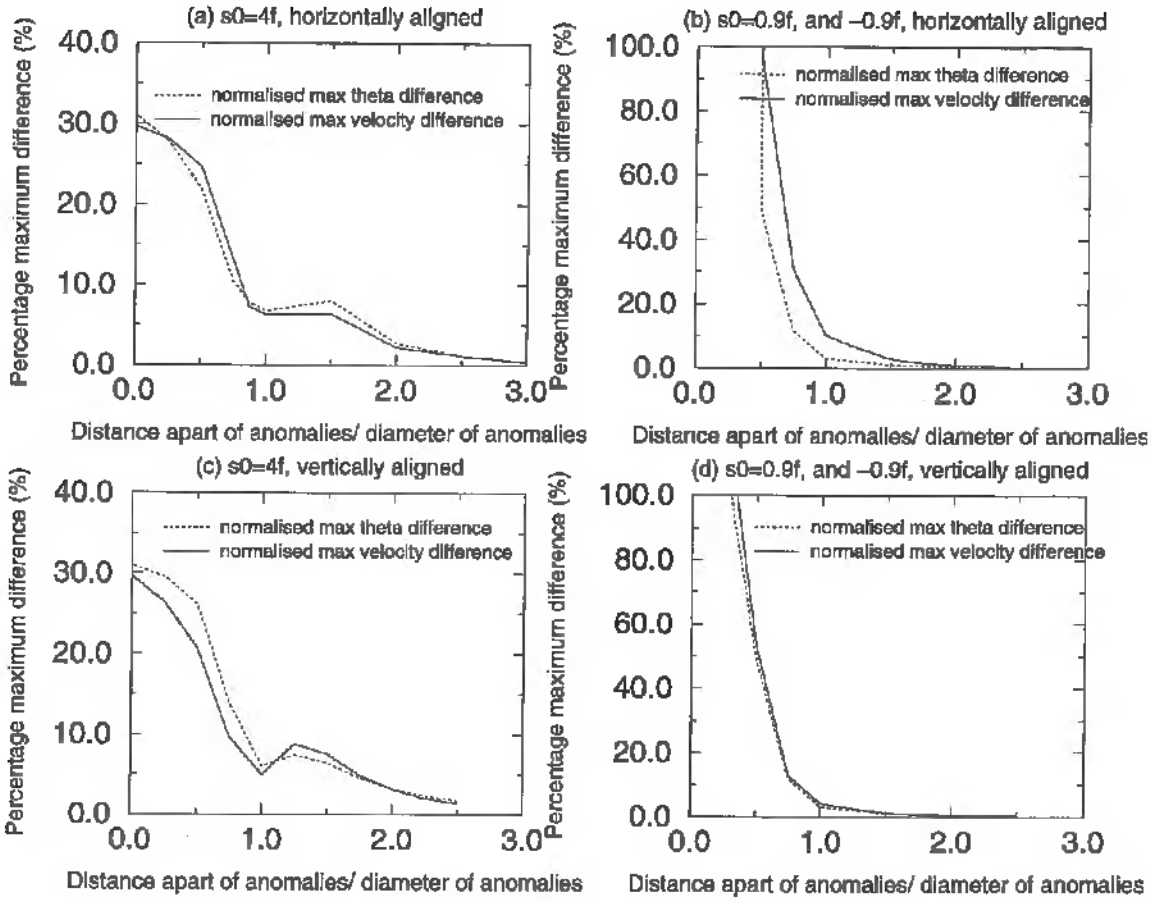

Fig 3: Percentage maximum difference between linearly superposed and full solutions for two anomalies at different distances apart with alignment and magnitude as stated on each graph. Note: the distance apart of the anomalies refers to the distance between the centres of the two anomalies.

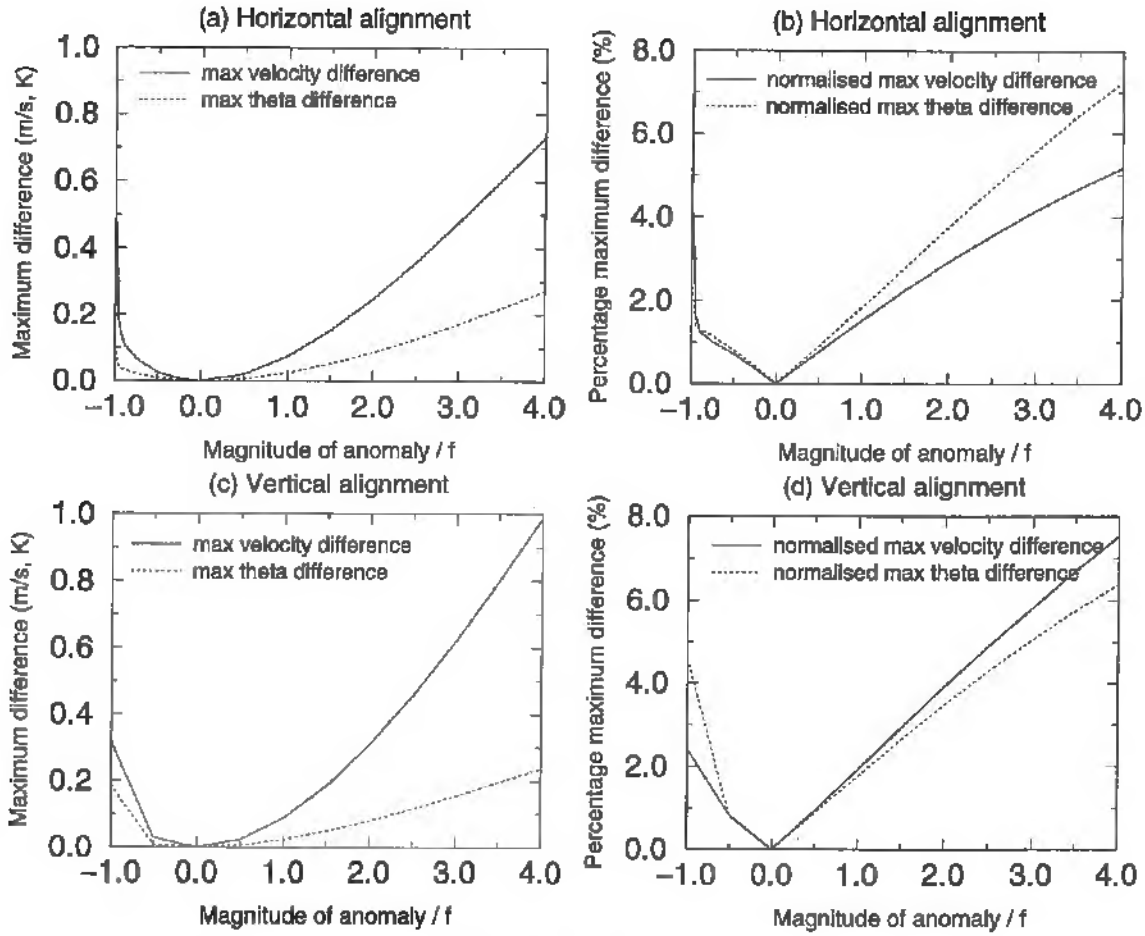

Fig 4: a) and c) Maximum, b) and d) percentage maximum, difference between linearly superposed and full solutions for different magnitude anomalies whose centres are 1.5 diameters apart, a) and b) horizontally, c) and d) vertically.

CURRENT JCMM INTERNAL REPORTS

This series of JCMM Internal Reports, initiated in 1993, contains unpublished reports and also versions of articles submitted for publication. The complete set of Internal Reports is available from the National Meteorological Library on loan, if required.

1. **Research Strategy and Programme**
   K A Browning et al
   January 1993

2. **The GEWEX Cloud System Study (GCSS)**
   GEWEX Cloud System Science Team
   January 1993

3. **Evolution of a mesoscale upper tropospheric vorticity maximum and comma cloud from a cloud-free two dimensional potential vorticity anomaly**
   K A Browning
   January 1993

4. **The Global Energy and Water Cycle**
   K A Browning
   July 1993

5. **Structure of a midlatitude cyclone before occlusion**
   K A Browning and N Roberts
   July 1993

6. **Development in Systems and Tools for Weather Forecasting**
   K A Browning and G Szejwach
   July 1993

7. **Diagnostic study of a narrow cold frontal rainband and severe winds associated with a stratospheric intrusion**
   K A Browning and R Reynolds
   August 1993

8. **Survey of perceived priority issues in the parametrizations of cloud-related processes in GCMs**
   K A Browning
   September 1993

9. **The Effect of Rain on Longwave Radiation**
   I Dharssi
   September 1993

10. **Physical Cloud Microprocesses - A Description of the Parametrization used in the Large Eddy Model**
    H Swann
    July 1994

11. **An Appreciation of the Meteorological Research of Ernst Kleinschmidt**
A J Thorpe
May 1992

12. **Potential Vorticity of Flow Along the Alps**
A J Thorpe, H Volkert and Dietrich Heimann
August 1992

13. **The Representation of Fronts**
A J Thorpe
January 1993

14. **A Parametrization Scheme for Symmetric Instability: Test for an Idealised Flow**
C S Chan and A J Thorpe
February 1993

15. **The Fronts 92 Experiment: a Quicklook Atlas**
Edited by T D Hewson
November 1993

16. **Frontal wave stability during moist deformation frontogenesis**
Part 1. Linear wave dynamics
C H Bishop and A J Thorpe
May 1993

17. **Frontal wave stability during moist deformation frontogenesis**
Part 2. The suppression of non-linear wave development
C H Bishop and A J Thorpe
May 1993

18. **Gravity waves in sheared ducts**
C Bishop and A J Thorpe
November 1993

19. **Potential Vorticity and the Electrostatics Analogy: Quasi-Geostrophic Theory**
C Bishop and A J Thorpe
November 1993

20. **Recent Advances in the Measurement of Precipitation by Radar**
A J Illingworth - April 1993

21. **Micro-Physique et Givrage. Cloud Microphysics and Aircraft Icing**
A J Illingworth May 1993

22. **Differential Phase Measurements of Precipitation**
M Blackman and A J Illingworth
May 1993

23. **Estimation of Effective Radius of Cloud Particles from the Radar Reflectivity**
N I Fox and A J Illingworth
May 1993

24. **A Simple Method of Dopplerising a Pulsed Magnetron Radar**
A Hau, A J Illingworth and J Eastment
November 1993

25. **Radiation and Polar Lows**
George C Craig
February 1994

26. **Collected preprints submitted to the International Symposium on the Life Cycles of Extratropical Cyclones; Bergen, Norway, 27 June - 1 July 1994**
April 1994

27. **Convective Frontogenesis**
Douglas J Parker and Alan J Thorpe
April 1994

28. **Improved Measurement of the Ice Water Content in Cirrus Using a Total Water Evaporator**
Philip R A Brown and Peter N Francis
April 1994

29. **Mesoscale Effects of a Dry Intrusion within a Vigorous Cyclone**
K A Browning and B W Golding
April 1994

30. **GEWEX Cloud System Study, Science Plan**
May 1994

31. **Parametrization of Momentum Transport by Convectively Generated Gravity Waves**
R Kershaw
February 1995

32. **Mesoscale Modelling Newsletter No 5**
May 1994

33. **Observations of the mesoscale sub-structure in the cold air of a developing frontal cyclone**
K A Browning, S A Clough, C S A Davitt, N M Roberts and T D Hewson
May 1994

34. **Longwave Radiative Forcing of a Simulated Tropical Squall Line**
Imtiaz Dharssi
July 1994

35. **On the nature of the convective circulation at a kata-cold front**
K A Browning
September 1994

36. **Collective preprints of papers submitted to the COST-75 International Seminar on Advanced Weather Radar Systems, Brussels, 20-23 September 1994**
November 1994

37. **Use of satellite imagery to diagnose events leading to frontal thunderstorms: Parts 1 and 11 of a case study**
K A Browning and N M Roberts
November 1994

38. **The role of spaceborne millimetre-wave radar in the global monitoring of ice cloud**
P R A Brown, A J Illingworth, A J Heymsfield, G M McFarquahar, K A Browning and M Gosset
December 1994

39. **Potential Vorticity Inversion**
Michael Ziemianski
October 1994

40. **Theory of mature tropical cyclones; a comparison between Kleinschmidt (1951) and Emanuel (1986)**
Suzanne L Gray
December 1994

41. **Dispersion and removal of pollutants during the passage of an atmospheric frontal System**
N R Gimson
December 1994

42. **The role of snow sublimation in frontogenesis**
D J Parker and A J Thorpe
December 1994

43. **Potential vorticity and the electrostatics Analogy: Ertel- Rossby formulation**
A J Thorpe and C H Bishop
December 1994

44. **Mesoscale aspect of extratropical cyclones: an observational perspective**
K A Browning
January 1995

45. **A Polar Low Outbreak: Evolution and Mesoscale Structures**
T D Hewson, G C Craig and C Claud
February 1995

46. **Generation of near-surface gusts of deep convection**
K Nakamura and R Kershaw
April 1995

47. **Attribution Concepts applied to the Omega Equation**
S A Clough, C S A Davitt and A J Thorpe
June 1995

48. **Parametrization of mixed-phase cloud and precipitation**
Susan P Ballard and M Gerard Hutchinson
June 1995

49. **Short-range forecasting of stratocumulus: Initialization Prediction**
Susan Ballard, Simon D Jackson and B Macpherson
June 1995

50. **Contributions of the JCMM/Dept of Meteorology Radar Group to the 27th AMS Radar Meteorology Conference, Vail October 1995**
June 1995

51. **Cold Pools in Shear**
Douglas J Parker
September 1995

52. **High-resolution analysis of frontal fracture**
K A Browning, S P Ballard and C S A Davitt
September 1995

53. **The Albedo of Broken Cloud Fields: Calculations using a modified two stream radiation code**
Imtiaz Dharssi and Roy Kershaw
October 1995

54. **Parametrization of momentum transport by convection. I: Theory and cloud modelling results**
P Kershaw and D Gregory
November 1995

55. **Variation of frontal structure along a cold front**
K A Browning and N M Roberts
November 1995

56. **Secondary Frontal Waves**
Douglas Parker
December 1995

57. **Objective Fronts**
T D Hewson
March 1996

58. **Mesoscale analysis of the activation of a cold front during cyclogenesis**
K A Browning, N M Roberts and A J Illingworth
June 1996

59. **Investigation of Different Representations of Rain in a 1-d Evaporation Model**
H Swann
May 1996

60. **Parametrization of diabatic processes in the inversion of the omega-equation**
M Athanassiadou and A J Thorpe

61. **The Role of the Environmental Flow in the Development of Secondary Frontal Cyclones**
I A Renfrew, A J Thorpe and A Joly
June 1996

62. **Consequences of the geostrophic momentum approximation on barotropic instability**
S Malardel, A J Thorpe and A Joly
June 1996

63. **Contributions to the AMS/RMS Conference on Mesoscale Processes**
Reading, 9-13 September 1996

64. **Vorticity and Potential Vorticity in Stratified Flows Interacting with an Isolated Obstacle**
Jorge A Gutierrez and A J Thorpe
September 1996

65. **Triple Point Development: Two Case Studies**
Douglas Parker
September 1996

66. **Radar observations of wind-shear splitting within evolving atmospheric Kelvin-Helmholtz billows**
D Chapman and K A Browning
April 1997

67. **Cold Frontal Structure derived from radar wind profilers**
K A Browning, D Jerrett, J Nash, T Oakley, N M Roberts
May 1997

68. **The dry intrusion and its effect on the frontal, cloud and precipitation structure of extratropical cyclones**
K A Browning - Text of invited special lecture at the Spring Conference of the Meteorological Society of Japan, University of Tsukuba, 22 May 1997

69. **Met. Office Unified Model data, diagnostic graphics programs, and other observational data available from the JCMM through the aegis of the Universities Weather Research Network UWERN.** Plus supplement.
Peter Panagi and Ed Dicks
June 1997

70. **Contributions of the JCMM/Dept of Meteorology Radar Group to 28th AMS Radar Meteorology Conference.** Austin, Texas, September 1997

71. **Sensitivity of short-range weather forecasts to local potential vorticity modifications**
Meral Demirtas and Alan Thorpe
July 1997

72. **Objective identification of frontal wave cyclones**
T D Hewson
August 1997

73. **Attribution and its application to mesoscale structure associated with tropopause folds**
A J Thorpe
September 1997

74. **The Role of the Environmental Flow in the Development of Secondary Frontal Cyclones**
Ian A Renfrew, Alan J Thorpe and Craig H Bishop
September 1997

75. **Potential Vorticity: A short history of its definitions and uses**
Alan J Thorpe and Hans Volkert
September 1997

76. **Superposing Semi-Geostrophic Potential Vorticity Anomalies**
H R Birkett and A J Thorpe
September 1997

Met Office Joint Centre for Mesoscale Meteorology Department of Meteorology
University of Reading PO Box 243 Reading RG6 6BB United Kingdom
Tel: +44 (0)118 931 8425 Fax: +44 (0)118 931 8791
www.metoffice.com